J|A|C|S
ARTICLES
Published on Web 09/21/2002

Synthesis, Structure, and Photochemistry of Exceptionally Stable Synthetic DNA Hairpins with Stilbene Diether Linkers

Frederick D. Lewis,* Yansheng Wu, and Xiaoyang Liu

Contribution from the Department of Chemistry, Northwestern University, Evanston, Illinois 60208-3113

Received May 17, 2002

Abstract: The structure and properties of 18 hairpin-forming bis(oligonucleotide) conjugates possessing stilbene diether linkers are reported. Conjugates possessing bis(2-hydroxyethyl)stilbene 4,4′-diether linkers form the most stable DNA hairpins reported to date. Hairpins with as few as two T:A base pairs or four noncanonical G:G base pairs are stable at room temperature. Increasing the length of the hydroxyalkyl groups results in a decrease in hairpin thermal stability. On the basis of the investigation of their circular dichroism spectra, all of the hairpins investigated adopt B-DNA structures, except for a hairpin with a short poly(G:C) stem which forms a Z-DNA structure. Both the strong fluorescence of the stilbene diether linkers and their trans−cis photoisomerization are totally quenched in hairpins possessing neighboring T:A and G:C base pairs. Quenching is attributed to an electron-transfer mechanism in which the singlet stilbene serves as an electron donor and T or C serves as an electron acceptor. In contrast, in denatured hairpins and hairpins possessing neighboring G:G base pairs the stilbene diether linkers undergo efficient photoisomerization.

Introduction

Bis(oligonucleotide) conjugates with synthetic linkers connecting short complementary oligonucleotides are known to form synthetic DNA or RNA hairpins which are, in some cases, more stable than natural hairpins possessing nucleotide linkers.[1] Letsinger and Wu[2] reported the use of a stilbenedicarboxamide (**Sa**, Chart 1) linker which formed stable hairpin structures possessing as few as three T:A or two G:C base pairs. At the time of their reported synthesis, the **Sa**-linked structures were the most stable mini-DNA hairpins known. The ability of the **Sa** linker to serve as an *electron acceptor* has been exploited in our studies of hole injection and migration processes in synthetic DNA hairpins.[3]

The search for a linker that would serve as an *electron donor* led us to investigate synthetic hairpins with stilbene diether (**Sd**, Chart 1) linkers. The linker **Sd2** which possesses hydroxyethyl substituents proved to form exceptionally stable synthetic hairpins with poly(T:A) stems.[4] The crystal structure of a **Sd2**-linked hairpin possessing six base pairs has been reported,[4] as has the one-way cis−trans photoisomerization in **Sd2**-linked hairpins.[5] We report here the preparation of 18 stilbene diether-linked hairpins (Chart 2) and the study of their structure, thermal stability, fluorescence, and photoisomerization. These properties are found to be dependent upon the length of the hydroxyalkyl substituent as well as the number and identity of the base pairs. The formation of stable hairpins possessing as few as two A:T, two G:C, or four G:G base pairs is observed. All of the hairpins have circular dichroism (CD) spectra characteristic of B-form structures except for a G_3−**Sd2**−C_3 hairpin which has a characteristic Z-form CD spectrum. Linker fluorescence and photoisomerization efficiencies are strongly dependent upon the identity of the neighboring base pair.

Chart 1. Structures of Stilbenedicarboxamide (**Sa**) and Stilbene Diether (**Sd**) Diol Linkers

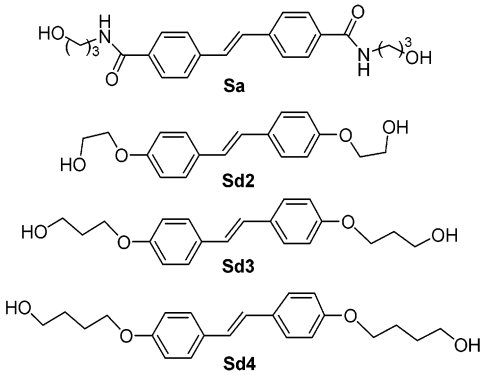

* To whom correspondence should be addressed. E-mail: lewis@chem.northwestern.edu.

(1) (a) Bevers, S.; Schutte, S.; McLaughlin, L. W. *J. Am. Chem. Soc.* **2000**, *120*, 11004−11005. (b) Durand, M.; Chevrie, K.; Chassignol, M.; Thuong, N. T.; Maurizot, J. C. *Nucleic Acids Res.* **1990**, *18*, 6353−6359. (c) Ma, M. Y. X.; McCallum, K.; Climie, S. C.; Kuperman, R.; Lin, W. C.; Sumner-Smith, M.; Barnett, R. W. *Nucleic Acids Res.* **1993**, *21*, 2585−2589. (d) Salunkhe, M.; Wu, T.; Letsinger, R. L. *J. Am. Chem. Soc.* **1992**, *114*, 8768−8772.
(2) Letsinger, R. L.; Wu, T. *J. Am. Chem. Soc.* **1995**, *117*, 7323−7328.
(3) (a) Lewis, F. D.; Letsinger, R. L.; Wasielewski, M. R. *Acc. Chem. Res.* **2001**, *34*, 159−170. (b) Lewis, F. D.; Wu, Y. *J. Photochem. Photobiol., C* **2001**, *2*, 1−16. (c) Lewis, F. D.; Liu, J.; Liu, X.; Zuo, X.; Hayes, R. T.; Wasielewski, M. R. *Angew. Chem., Int. Ed.* **2002**, *41*, 1026−1028. (d) Lewis, F. D.; Zuo, X.; Liu, J.; Hayes, R. T.; Wasielewski, M. R. *J. Am. Chem. Soc.* **2002**, *124*, 4568−4569.
(4) Lewis, F. D.; Liu, X.; Wu, Y.; Miller, S. E.; Wasielewski, M. R.; Letsinger, R. L.; Sanishvili, R.; Joachimiak, A.; Tereshko, V.; Egli, M. *J. Am. Chem. Soc.* **1999**, *121*, 9905−9906.
(5) Lewis, F. D.; Liu, X. *J. Am. Chem. Soc.* **1999**, *121*, 11928−11929.

Chart 2. Structures of Stilbene Diether-Linked Conjugates in Their Hairpin Conformations, Showing Hydrogen Bonding between Canonical (---) and Noncanonical (|||) Base Pairs

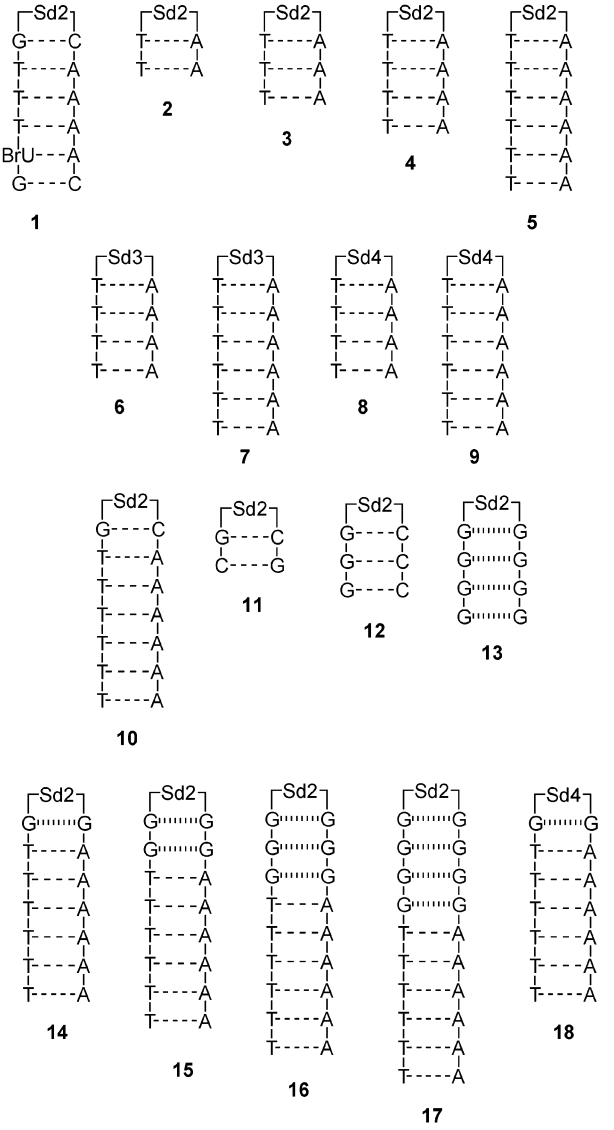

Results

Bis(*n*-hydroxyalkyl)stilbene 4,4′-Diethers. The stilbene diethers **Sd2**, **Sd3**, and **Sd4** were prepared by the method of Sieber.[6] Their MM2-minimized structures consist of a nearly planar rodlike stilbene with appended flexible hydroxyalkyl groups. The hydroxyalkyl groups in **Sd2** adopt the gauche conformation favored by ethylene glycol monomethyl ether,[7] whereas the hydroxyalkyl groups in **Sd3** and **Sd4** adopt lowest energy fully extended trans conformations which are only slightly more stable than the gauche conformations (Chart 1). The distances between the two hydroxy oxygen atoms are 17.0, 21.4, and 23.7 Å for **Sd2**, **Sd3**, and **Sd4**, respectively.

The absorption spectra of **Sd3** in methanol and 1:10 methanol/water are shown in Figure 1, and the absorption maxima of the stilbene diethers are reported in Table 1. The spectra in methanol solution consist of a single allowed, long-wavelength absorption band, similar to that for 4,4′-dimethoxystilbene.[8] Thus, the hydroxyalkyl groups do not influence the spectra in methanol solution. The absorption spectra in tetrahydrofuran are identical to those in methanol. The stilbene diethers are insoluble in water and sparingly soluble in methanol−water. Their absorption spectra in methanol−water display a blue-shift in the absorption maxima and a red-shifted onset of absorption.

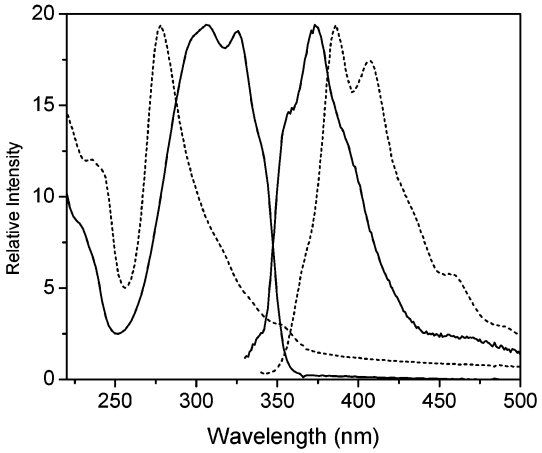

Figure 1. Absorption and fluorescence spectra of the stilbene diether **Sd3** in methanol (—) and methanol−water (---) solution.

Table 1. Absorption and Fluorescence Maxima for the Stilbene Diethers

	solvent	Sd2	Sd3	Sd4
λ_{abs}, nm	methanol	304, 326	304, 326	304, 326
	methanol−water	282	278	276
λ_{fl}, nm	methanol	374	374	374
Φ_{fl}[a]	methanol	0.21	0.22	0.22
τ_{fl}, ns[b]	methanol	0.35	0.37	0.37
λ_{fl}, nm	methanol−water	386	386, 409	409
Φ_{fl}[a]	methanol−water	0.02	0.06	0.06
τ_{fl}, ns[c]	methanol−water		1.9 (79), 6.7 (21)	0.87 (70), 5.9 (30)

[a] Fluorescence quantum yield in deoxygenated solution determined using quinine sulfate actinometry. [b] Fluorescence decay time obtained from single-exponential fits. [c] Fluorescence decay times and preexponentials (values in parentheses) obtained from dual exponential fits.

The fluorescence spectra of **Sd3** in methanol and methanol−water are also shown in Figure 1, and the fluorescence maxima, quantum yields, and decay times of the stilbene diethers are reported in Table 1. The fluorescence parameters for the stilbene diethers are similar to those of 4,4′-dimethoxystilbene in methanol ($\Phi_{fl} = 0.20$, $\tau_{fl} = 0.42$ ns).[9] The fluorescence decay time for the stilbene diethers are near the time resolution of our lifetime apparatus (ca. 0.5 ns). The fluorescence spectra are red-shifted in methanol−water. The fluorescence quantum yields in methanol−water are smaller than those in methanol. The fluorescence decay in methanol−water is best fit by a dual exponential function in which both decay components are longer lived than the single component decay obtained in methanol solution (Table 1). The band shapes of the fluorescence of **Sd3** and **Sd4** are independent of temperature below 70 °C but resemble the spectra obtained in methanol at 90 °C.

Irradiation of **Sd2** with 344 nm light in methanol or dimethyl sulfoxide solution results in photoisomerization, yielding a mixture of **Sd2** and its cis isomer, *c*-**Sd2** (eq 1). The photo-

(6) Sieber, R. H. *Liebigs Ann. Chem.* **1969**, *730*, 31−46.
(7) Eliel, E. L.; Wilen, S. H. *Stereochemistry of Organic Compounds*; Wiley: New York, 1994.
(8) Lewis, F. D.; Bedell, A. M.; Dykstra, R. E.; Elbert, J. E.; Gould, I. R.; Farid, S. *J. Am. Chem. Soc.* **1990**, *112*, 8055−8064.
(9) Zeglinski, D. M.; Waldeck, D. H. *J. Phys. Chem.* **1988**, *92*, 692−701.

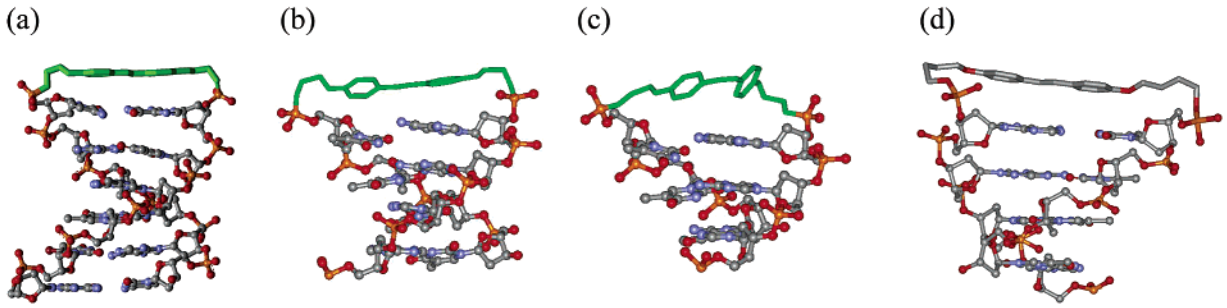

Figure 2. (a) Crystal Structure of the **Sd2**-linked hairpin **1** and MM2-minimized structures of conjugates **4** (b), *c*-**4** (c), and **8** (d). Hairpin linkers are at the top of the structures.

stationary state obtained upon irradiation of either isomer is 28% **Sd2** and 82% *c*-**Sd2**. Quantum yields measured by comparison with the secondary standard *trans*-stilbene are shown in eq 1.[10]

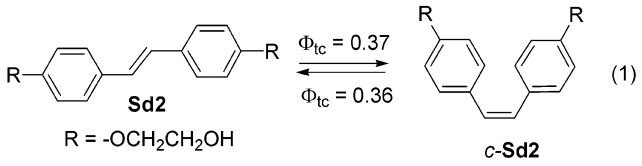

(1)

Synthesis and Structure of Stilbene Diether-Linked Hairpins. Prior to incorporation of the stilbene diethers into a synthetic (bis)oligonucleotide conjugate, they were converted to the monoprotected, monoactivated diol by sequential reaction with 4,4′-dimethoxytrityl chloride and with 2-cyanoethyl diisopropylchlorophosphoramidite (see Experimental Section). The conjugates **1**−**18** shown in Chart 2 were prepared by means of conventional phosphoramidite chemistry using a Millipore Expedite oligonucleotide synthesizer following the procedure developed by Letsinger and Wu.[2] The conjugates were first isolated as trityl-on derivatives by RP HPLC, then detritylated in 80% acetic acid for 30 min, and then repurified by RP HPLC. A single peak was detected by both RP and IE HPLC. Molecular weights of representative conjugates were determined by electrospray ionization mass spectroscopy.

Irradiation of hairpin **4** under denaturing conditions in 50% ethanol−water results in conversion to a mixture of **4** and a single photoproduct formed in 72% yield. Formation of secondary photoproducts was observed after the photostationary state was attained. Irradiation under denaturing conditions in water at pH > 12 resulted in more complex product mixtures. The product of irradiation in ethanol−water was isolated by HPLC and identified as the cis isomer, *c*-**4**, by comparison of its absorption spectrum with that of *c*-**Sd2** (eq 1) and by its photoisomerization in ethanol−water to yield the same mixture of isomers as obtained from **4**.

The crystal structure of the bromine-labeled conjugate **1** obtained by crystallization from solutions containing Sr^{2+} ions has previously been reported.[4] The asymmetric unit consists of four **Sd2**-linked hairpins in which the stilbenes form an edge-to-face tetramer. The structure of one hairpin from the unit cell is shown in Figure 2a. The base pairs adopt a standard B-form DNA conformation, and the linker is π-stacked with the adjacent G:C base pair. Both ethylenes in the linker adopt gauche conformations, as is the case for 1,2-dimethoxyethane and poly(ethylene oxide).[7] This results in a rather short end-to-end distance for the linker; the average distance between its outer oxygen atoms is ca. 16.5 Å, similar to that calculated for the **Sd2** diol (Chart 1). The average interstrand distance between phosphorus atoms bound to the **Sd2** linker is 18.1 Å and thus comparable to the average distance of 17.7 Å for phosphorus atoms from opposite strands in all other dimer steps. Details of the crystal structure will be reported elsewhere.

The MM2-minimized structure for conjugate **1** has a hairpin geometry similar to that for the crystal structure. The other conjugates in Chart 2 can also adopt minimized structures in which the linker serves as the loop in a B-DNA hairpin structure. Hairpin formation is consistent with the results of UV thermal dissociation studies and circular dichroism (CD) spectra (vide infra). The minimized structures for conjugates **4**, *c*-**4**, and **8** are shown in Figure 2b−d. The minimized structure for **4** (Figure 2b), which possesses a **Sd2** linker, has a loop region similar to that of conjugate **1**. The structure for *c*-**4** (Figure 2c) has a severely distorted loop region. The minimized structures for conjugates **6** and **8** (Figure 2d) have wider loop regions in which the alkyl groups extend beyond the sugar−phosphate backbone. However, the stilbene diether chromophores remain π-stacked with the neighboring T:A base pair.

Ultraviolet Spectra and Thermal Dissociation. The ultraviolet absorption spectra of the stilbene diether-linked conjugates display a long-wavelength absorption band ($\lambda_{max} \sim 327$ nm) assigned to the stilbene π,π^* transition and a shorter wavelength band ($\lambda_{max} \sim 260$ nm) assigned to overlapping stilbene and nucleobase absorption bands. The long wavelength bands are slightly red-shifted with respect to that of the stilbene diether, as shown in Figure 3 for conjugate **4**.

The 260 nm bands display an increase in absorbance (hyperchromism) upon heating in aqueous buffer containing 0.1 M NaCl, whereas the 327 nm bands display a decrease in absorbance. Thermal dissociation profiles for the **Sd2**-linked hairpins **2**−**5** (2×10^{-6} M) in 0.1 M NaCl aqueous buffer (10 mM sodium phosphate, pH 7.2) are shown in Figure 4. The first derivatives of these curves provide the melting temperatures (T_m) reported in Table 2. The values of T_m for **2**−**5** increase with increasing length of the polyT−polyA sequences and with increasing salt concentration. However, they are independent of conjugate concentration, indicative of the formation of hairpin rather than duplex structures. The T_m of hairpin **4** is higher in 1.0 M NaCl (60.8 °C) and lower in water (50.8 °C) than in 0.1 M NaCl (54.0 °C). Lower T_m values are also observed in ethanol−water mixtures (50.0, 37.6, and 22.2 °C , in 10, 30, and 50% ethanol, respectively). The T_m values for *c*-**4** are

(10) Lewis, F. D.; Johnson, D. E. *J. Photochem.* **1977**, *7*, 421−423.

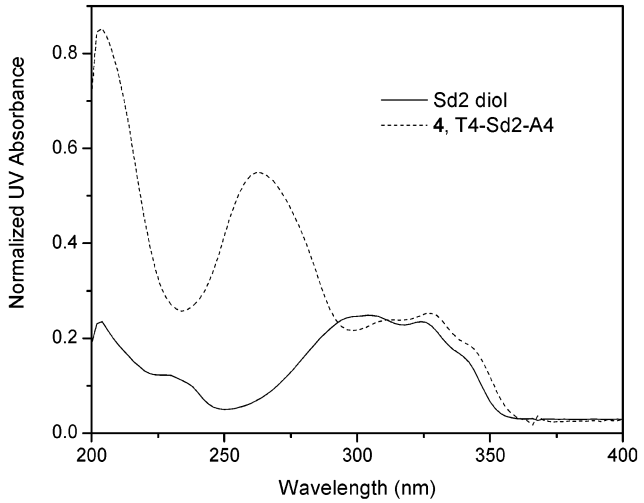

Figure 3. Absorption spectra of the stilbene diether **Sd2** in methanol solution and the **Sd2**-linked conjugate **4** in aqueous 0.1 M NaCl.

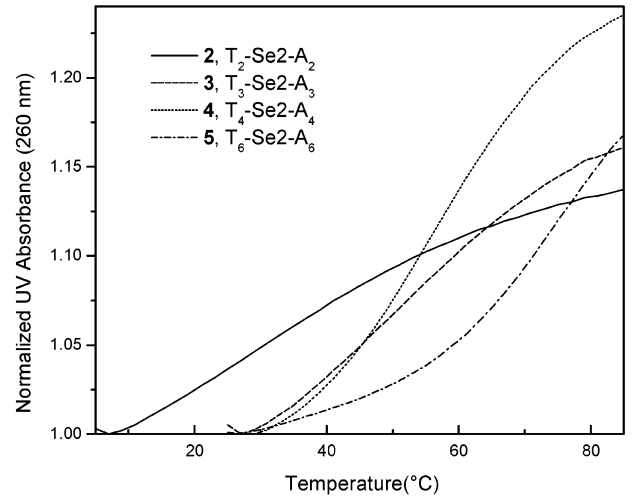

Figure 4. Thermal dissociation profiles for the **Sd2**-linked conjugates **2**−**5**.

Table 2. Melting Temperatures for Stilbene Diether-Linked Hairpins[a]

hairpin	T_m, °C	hairpin	T_m, °C
1	78.4	**10**	72.4
2	30 (33)	**11**	>80
3	46.7 (48.9)	**12**	>80
4	54.0 (60.8)	**13**	48.8
c-**4**	30 (33)	**14**	53.4
5	64.2 (73.1)	**15**	49.8
6	53	**16**	46.5
7	66.3	**17**	47.7
8	48.3	**18**	50.2
9	56.6		

[a] Values for 2×10^{-6} M conjugates in standard buffer (10 mM sodium phosphate, pH 7.2) containing 0.1 M NaCl or 1.0 M NaCl (values in parentheses).

significantly lower than those of **4**, in 1.0 M NaCl (33 °C), 0.1 M NaCl (30 °C), and 30% ethanol−water (26 °C).

Conjugates **1** and **10** possess a combination of G:C and A:T base pairs. Their melting transitions are above 70 °C in 0.1 M aqueous NaCl. Since these conjugates are related to conjugate **5** by the replacement of two A:T base pairs with G:C base pairs in the case of **1** and by the addition of one G:C base pair in the case of **10**, it is not surprising that their T_m values are appreciably higher than that of **5** (Table 2). Conjugates **11** and **12** possess only GC base pairs. No hyperchromism is observed upon heating either conjugate from 10 to 60 °C in aqueous 0.1 M NaCl or upon heating **11** in water or 50% ethanol−water. Hyperchromism is observed at temperatures >60 °C, as previously observed by Letsinger and Wu[2] for analogous **Sa**-linked hairpins. These results are indicative of values of T_m > 80 °C.

Conjugate **13** contains two polyG arms. A freshly prepared dilute solution of conjugate **13** (2×10^{-6} M) displays reversible melting with a T_m value of 48.8 °C. Annealing of **13** at 85 °C followed by slow cooling to room temperature results in a change in the melting behavior indicative of the formation of a more stable G-quadruplex or aggregate structures which are also obtained at higher concentrations of **13**. Conjugates **14**−**18** possess G:G mismatches inserted between the stilbene diether linker and a T_6:A_6 duplex region. The values of T_M for these conjugates are lower than that of hairpin **5**; however, their thermal dissociation profiles are similar in appearance to that of **5**. The melting profiles for **14**−**18** are reversible and do not change upon annealing. The value of T_M decreases with the number of G:G mismatch base pairs for **14**−**16** but increases slightly for **17**. The value of T_M is lower for conjugate **18**, which possesses an **Sd4** linker, than for **14,** which possesses an **Sd2** linker.

Circular Dichroism Spectra. The circular dichroism (CD) spectra of conjugates **2**−**4** which possess poly(T:A) stems are shown in Figure 5a. The spectra of **4** and **5** have a positive band at 283 nm and a negative band at 250 nm, consistent with formation of a B-form DNA structure in solution. The CD spectra of **2** and **3** are similar but are broader and have red-shifted minima. A very weak negative band is observed at longer wavelength (300−350 nm). The CD spectrum of conjugate **9** is similar to that of **4** except that no long-wavelength band (>300 nm) is detected.

The CD spectrum of **11** (Figure 5b), which possesses two G:C base pairs, is similar in appearance to that of **2** (Figure 5a). However, its 254 nm minimum and 291 nm maximum are red-shifted with respect to those of **2**, and the long-wavelength minimum at 340 nm is more pronounced. The CD spectrum of conjugate **12** either in water or in standard buffer (Figure 5b) is markedly different from that of the poly(T:A) hairpins, displaying a positive peak at 260 nm and a negative peak at 281 nm characteristic of the left-hand helical conformation of Z-form DNA. The CD spectrum of conjugate **13** (Figure 5c), which possesses only noncanonical G:G base pairs, is similar to that of the poly(T:A) hairpin **4**. This is also the case for conjugates **14** and **15**, which possess one and two G:G base pairs, respectively. At higher concentrations, the CD spectrum of **13** is more complex, indicative of the formation of G-quadruplex structures; however, the CD spectra of **14** and **15** are not concentration dependent.

Conjugate Fluorescence and Photoisomerization. The hairpins **1**−**12** are very weakly fluorescent ($\Phi_f < 10^{-3}$). The weak fluorescence is attributed to quenching of the strong stilbene diether fluorescence (Table 1) by the neighboring A:T or G:C base pair.[4] In contrast, relatively strong fluorescence is observed for the hairpins **13**−**17**, which possess one or more G:G base pairs adjacent to the stilbene diether linker. The fluorescence excitation and emission spectra of **13** (Figure 6) are similar to those of the stilbene diether linkers in methanol solution (Figure 1). Fluorescence data for **13**−**17** are sum-

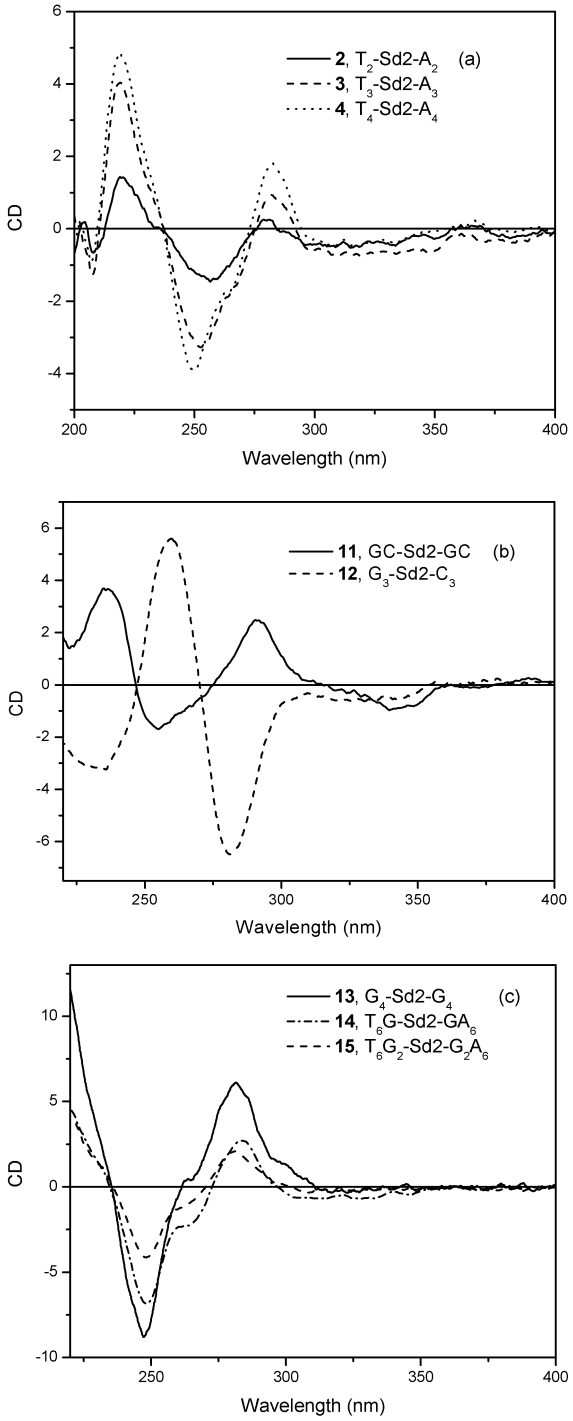

Figure 5. Circular dichroism spectra of 2×10^{-6} M conjugates in aqueous buffer (0.1 M NaCl, 10 mM sodium phosphate): (a) conjugates **2**−**4**; (b) conjugates **11** and **12**; (c) conjugates **13**−**15**.

marized in Table 3. Fluorescence quantum yields and decay times for hairpins **16** and **17** are similar to the values for the diol **Sd2** in methanol solution. Both quantum yields and decay times decrease for **15** and **14**, which have fewer G:G base pairs. Dual exponential fluorescence decay is observed for hairpin **13**; however, the short-lived component accounts for 96% of the fluorescence intensity and has a decay time similar to those of **16** and **17**.

As described above, irradiation of denatured **4** (50% ethanol−water, 25 °C) results in formation of a mixture of **4** and *c*-**4**.

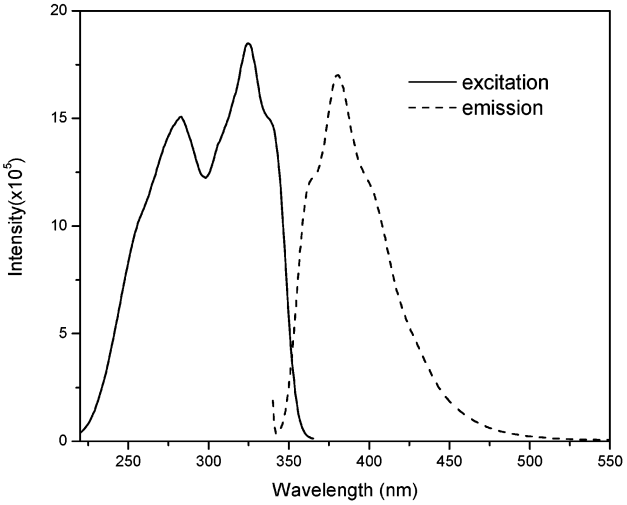

Figure 6. Fluorescence excitation and emission spectra of conjugate **13** in standard buffer.

Table 3. Fluorescence Data for Hairpins with G:G Base Pairs[a]

hairpin	Φ_{fl}[b]	τ_s, ns[c]
13	0.17 ± 0.01	0.92 (96%), 4.1 (4%)
14	0.12 ± 0.02	0.32 ± 0.1
15	0.19 ± 0.01	0.53 ± 0.03
16	0.24 ± 0.01	0.69 ± 0.05
17	0.24 ± 0.01	0.69 ± 0.05

[a] Data for deoxygenated 2×10^{-6} M solutions in standard buffer. [b] Fluorescence quantum yields determined using quinine sulfate actinometry. [c] Single- or double-exponential decay times (preexponentials in parentheses).

Quantum yields for reversible isomerization of **4** and *c*-**4** are $\Phi_{tc} = 0.19$ and $\Phi_{ct} = 0.10$. No isomerization is observed when **4** is irradiated in standard buffer (0.1 M NaCl, 10 mM sodium phosphate, pH 7.2). In contrast, irradiation of *c*-**4** results in quantitative (>95%) conversion to **4** under conditions where it is either partially denatured (30% ethanol−water, 25 °C) or fully base-paired (0.1 M NaCl, 25 °C, $\Phi_{ct} = 0.17$). Trans−cis isomerization results in bleaching of the 327 nm band assigned to the *trans*-stilbene diether linker. Thus, the occurrence of isomerization can be qualitatively evaluated by monitoring the 327 nm absorption during irradiation. During the time required for quantitative conversion of *c*-**4** to **4** in 0.1 M NaCl, no bleaching of the 327 band is observed for hairpins with A:T or G:C base pairs adjacent to the **Sd** linkers. However, rapid bleaching of the 327 band is observed for hairpins **13** and **17**, both of which have adjacent G:G base pairs.

Discussion

Stilbene Diethers. The absorption and fluorescence spectra (Figure 1), fluorescence quantum yields, and fluorescence decay times of the stilbene diethers **Sd2**−**4** (Table 1) are similar to those of 4,4′-dimethoxystilbene in methanol solution ($\Phi_{fl} = 0.20$, $\tau_{fl} = 0.42$ ns).[9] Thus, the hydroxyalkyl groups have little effect on the photophysical properties of the stilbene diethers in methanol solution. The stilbene diethers undergo reversible photoisomerization in methanol solution. The sum of the isomerization (eq 1) and fluorescence quantum yields is 0.93 ± 0.1, in accord with the usual mechanism for stilbene isomerization via a twisted singlet intermediate.[11] The absorption spectra of the stilbene diethers is broadened and its maximum

blue-shifted in aqueous solution, whereas the fluorescence spectrum is red-shifted (Figure 1). These changes are similar to those observed by Whitten and co-workers for stilbene aggregates in Langmuir−Blodgett (LB) films and attributed to exciton coupling in the H-aggregates.[12]

We assume that the stilbene diethers form laminar aggregates, similar to those of known bolaamphiphiles possessing aromatic cores and pendant hydroxyalkyl groups.[13] The fluorescence quantum yields of the stilbene aggregates in aqueous solution are lower than those of the isolated molecules in methanol solution; however, the fluorescence decay times are longer in aqueous solution (Table 1). The increased lifetimes can be attributed to an increased barrier for torsion about the stilbene double bond in the stilbene diether aggregates. The stilbene aggregates display remarkable thermal stability. Fluorescence melting studies indicate that the transition from aggregate to monomer occurs above 75 °C.

Hairpins with T:A Base Pairs. The thermal dissociation profiles and CD spectra of conjugates **2**−**9** indicate that they form hairpin structures with T:A base pairing between their polyT and polyA arms. Their CD spectra (Figure 5a) show negative and positive peaks near 250 and 283 nm, characteristic of B-DNA.[14] Even conjugate **2**, which can form only two T:A base pairs, displays significant hyperchromism with a derivative at 33 °C (Figure 4) and a room-temperature CD spectrum (Figure 5a) similar to those of its homologues **3**−**5**. Increasing the number of T:A base pairs in the series **2**−**5** results in an increase in the value of T_m (Table 2) and sharpening of the CD spectra (Figure 5a).

The T_m values of the hairpins **2**−**5** (Table 2) are higher than those of the analogous stilbenediamide-linked hairpins (Chart 1) reported by Letsinger and Wu.[2] Thus, the stilbene diether linkers form the most stable synthetic polyA-linker−polyT hairpins reported to date. To our knowledge, no DNA or RNA oligonucleotides have been reported to form hairpin structures with short poly(T:A) stems.[15] The exceptional stability of the **Sd2**-linked hairpins is, no doubt, related to the compact structure of the linker, as observed in the crystal structure of hairpin **1** in which the average plane-to-plane separation between the stilbene linker chromophore and adjacent G:C base pair is 3.25 Å, somewhat shorter than the 3.4 Å average base stacking distance in B-form DNA.[4] The π-stacking interaction can account for the red-shifted absorption of the linker chromophore (Figure 3) and the weak negative circular dichroism observed between 300 and 350 nm (Figure 5a). In view of the crystal structure of hairpin **1** it is somewhat surprising that the **Sd2**-linked hairpins display neither a strong induced CD spectrum nor a Cotton effect.[16] One possible explanation for the absence of strong induced circular dichroism is that the dihedral angle between the transition moments of the stilbene and adjacent base chromophores is near 0 or 180°, in which case the amplitude of the Cotton effect will vanish.[17]

Table 4. Thermodynamic Parameters for Hairpin Formation[a]

hairpin	solvent	T_m,[b] °C	$-\Delta G°_{298}$, kcal/mol	$-\Delta H°$, kcal/mol	$-\Delta S°$, cal/(mol·K)
4	0.1 M NaCl	54.0	2.5	23.2	69.5
	water	50.8	1.5	18.4	56.9
	30% EtOH−water	37.6	1.2	29.2	93.8
c-**4**	30% EtOH−water	26.1	0.08	22.9	76.3
8	0.1 M NaCl	48.3	1.5	21.1	65.7
13	0.1 M NaCl	48.8	2.8	37.4	116
14	0.1 M NaCl	53.4	2.5	28.5	87.1

[a] Determined from absorption data using the method of ref 19. [b] Data from Table 2.

The T_m values for hairpins **4** and **6**, which possess four A:T base pairs, and **5** and **7**, which possess six A:T base pairs, are similar (Table 2). Thus, increasing the length of the alkane chains in the stilbene diether linkers from two to three methylenes has little effect on the thermal stability of the hairpin. In contrast the T_m value for hairpin **8**, which possesses a **Sd4** linker, is lower than that of either **4** or **6**; however, its CD spectrum is similar to that of **4**. The minimized structure of **8** (Figure 2d) possesses a gauche−gauche turn in one of the tetramethylene linkers. The T_m value for hairpin **9**, which possesses a **Sd4** linker, is also significantly lower than that of either **5** or **7,** which possess **Sd2** or **Sd3** linkers, respectively. The T_m values of **8** and **9** are remarkably similar to those of the corresponding **Sa**-linked hairpins, which have the same number of atoms separating the two hydroxyl groups (Chart 1).[2] Thus, it appears that the geometry of the linker rather than its donor or acceptor properties determines the thermal stability of these synthetic hairpins. It is interesting to note that the melting temperatures of DNA hairpins with polyT loops decrease with the length of the loop.[18]

Thermodynamic parameters for formation of DNA hairpins can be readily obtained from analysis of the absorption spectral data using the method of Marky and Breslauer[19] in cases where the low- and high-temperature plateaus of the melting curve can be determined. This is not possible for conjugates **2** and **3** for which the melting transition occurs over a broad temperature range (Figure 4) or for conjugates with melting temperatures over 60 °C for which the high-temperature plateau is not resolved. Thermodynamic parameters for conjugates **4**, *c*-**4**, and **8** are reported in Table 4. The values of T_m for **4** decrease, and ΔG becomes less favorable, as expected, as the solvent is changed from 0.1 M NaCl to water or ethanol−water.[15] Reducing the salt concentration results in a less favorable $\Delta H°$, which is partially compensated by a more favorable $\Delta S°$. Addition of ethanol makes $\Delta H°$ more favorable and $\Delta S°$ less favorable, as previously reported by Hickey and Turner[20] for RNA duplex formation. The lower melting temperature of *c*-**4** versus **4** in 30% ethanol−water is largely a consequence of less favorable entropy, in accord with the distorted hairpin structure of *c*-**4** (Figure 2c). The lower melting temperature and less

(11) (a) Saltiel, J.; Sun, Y.-P. In *Photochromism, Molecules and Systems*; Duerr, H., Boaus-Laurent, H., Eds.; Elsevier: Amsterdam, 1990; pp 64−164. (b) Waldeck, D. H. *Chem. Rev.* **1991**, *91*, 415−436.
(12) (a) Whitten, D. G. *Acc. Chem. Res.* **1993**, *26*, 502−509. (b) Song, X.; Geiger, C.; Vaday, S.; Perlstein, J.; Whitten, D. G. *J. Photochem. Photobiol., A* **1996**, *102*, 39−45.
(13) (a) Hentrich, F.; Tschierske, C.; Diele, S.; Sauere, C. *J. Mater. Chem.* **1994**, *4*, 1547−1558. (b) Kölbel, M.; Beyersdorff, T.; Cheng, X. H.; Tschierske, C.; Kain, J.; Diele, S. *J. Am. Chem. Soc.* **2001**, *123*, 6809−6818.
(14) Bloomfield, V. A.; Crothers, D. M.; Tinoco, I. *Nucleic Acids. Structures, Properties, and Functions*; University Science Books: Sausalito, CA, 2000.
(15) Turner, D. H. In *Nucleic Acids. Structures, Properties, and Functions*; Bloomfield, V. A., Crothers, D. M., Tinoco, I., Eds.; University Science Books: Sausalito, CA, 2000.
(16) Ardhammar, M.; Kurucsev, T.; Nordén, B. In *Circular Dichroism*; Berova, N., Nakanishi, K., Woody, R. W., Eds.; Wiley: New York, 2000.
(17) Harada, N.; Nakanishi, K. *Circular Dichroic Spectroscopy*; University Science Books: Mill Valley, CA, 1983.
(18) Hilbers, C. W.; Haasnoot, C. A. G.; de Bruin, S. H.; Joordens, J. J. M.; Van Der Marel, G. A.; Van Boom, H. H. *Biochemie* **1985**, *67*, 685−695.
(19) Marky, L. A.; Breslauer, K. J. *Biopolymers* **1987**, *26*, 1601−1620.
(20) Hickey, D. R.; Turner, D. H. *Biochemistry* **1985**, *24*, 2086−2094.

favorable free energy for hairpin formation of **8** versus **4** is seen to be a consequence of less favorable enthalpy rather than an increase in entropy. The presence of a gauche−gauche turn in the minimized structure for **8** (Figure 2d) could account for its smaller (less negative) value of $\Delta H°$.

Hairpins with G:C Base Pairs. Hairpins **1** and **10**−**12** have melting temperatures >70 °C in 0.1 M NaCl (Table 2). The presence of G:C base pairs in **1** and **10** results in a more stable hairpin than the poly(T:A) hairpin **5**, which has a $T_m = 64.2$ °C. Hairpins **11** and **12** can form two or three G:C base pairs, respectively. An analogue of **11** possessing a stilbenediamide linker (Chart 1) connecting two G:C base pairs has a broad thermal dissociation profile with a $T_m \sim 60$ °C in aqueous 0.1 M NaCl.[2] Thus, the **Sd2**-linked hairpin **11** is more stable than the stilbenediamide-linked hairpin, as is the case for the poly(T:A) hairpins. Hairpin **11** is also more stable than DNA minihairpins with 5′GCGAAGC and related sequences.[21]

The CD spectrum of **11** (Figure 5b) is similar to those of the poly(A:T) hairpins which adopt B-form structures (Figures 5a). The induced circular dichroism of the **Sd2** linker in **11** is much stronger than that in **2**−**5**. This may reflect a stronger interaction of the stilbene chromophore with an adjacent G:C than with an adjacent A:T or better structural definition of the loop region with an adjacent G:C. The stilbene−G:C π-stacking distance observed in the crystal structure of hairpin **1** (Figure 2a) is, in fact, remarkably short (3.25 Å).[4] The CD spectrum of **12** (Figure 5b) is markedly different from those of **11** or the poly(A:T) hairpins and is similar to that of the Z-DNA duplex formed by the self-complementary hexanucleotide d(CGCGCG).[14] Alternating d(CG) sequences are commonly found to adopt Z-form duplex and hairpin structures.[22,23] While out-of-alternation Z-DNA structures are less common, the sequence d(CCCGGG) has been reported to adopt a Z-DNA structure.[22] Hairpin **12** presumably can adopt a base-paired geometry similar to that of d(CCCGGG) and thus provides the simplest model for a Z-DNA structure reported to date.

Hairpins with G:G Base Pairs. G:G forms the most stable mismatched base pair and is commonly encountered both in DNA and RNA.[24,25] The G:G base pair can adopt a number of structures, the syn−anti (Hoogsteen) being the most general for single G:G mismatches in B-DNA duplexes. While single G:G mismatches do not distort the π-stacking of B-DNA, they do distort the sugar geometry, leading to a decrease in duplex stability. Tandem G:G mismatches in duplex DNA have not been widely investigated due to the propensity of G-rich regions to form G-quadruplex structures.[25] An exception is provided by $d(GGGA)_n$ oligomers studied by Huertas and Azorín,[26] which form stable intramolecular hairpin structures stabilized by tandem G:G base pairs. These hairpins are moderately stable, having T_m values between 40 and 50 °C in 50 mM NaCl. The G:G base pair structure in these hairpins is not known; however, the N7 group of one of the two guanines is most likely involved.

Freshly deprotected dilute solutions of conjugate **13** form a monomeric hairpin structure in 0.1 M NaCl solution. The hairpin displays reversible melting, with a T_m (48.8 °C) similar to that reported for $d(GGGA)_n$ oligomers.[26] The CD spectrum of **13** (Figure 5c) is similar to that of the poly(T:A) hairpins (Figure 5a), which adopt B-DNA structures. Upon being annealed at 80 °C followed by slow cooling to room temperature, conjugate **13** forms an aggregate structure assigned to a parallel quadruplex on the basis of its CD spectrum.[27] The quadruplex does not display a melting transition below 85 °C. On the basis of this preliminary evidence, it seems likely that the monomeric hairpin is the kinetic product and the parallel quadruplex the thermodynamic product of base-pairing in **13**. The thermodynamic data for **13** (Table 4) indicate that it forms a slightly more stable hairpin than the poly(T:A) hairpin **4** as a consequence of a more favorable enthalpy of formation which is largely compensated by a less favorable entropy of formation. The more favorable enthalpy may reflect more extensive π-stacking overlap for the G:G vs T:A steps.

Introduction of a single G:G mismatch in hairpin **14** results in a lowering of T_m compared to that of hairpin **5** (53.4 vs 64.2 °C, Table 2). This decrease is similar to that observed for RNA duplex structures upon substitution of a G:G for a G:C base pair.[25] Thermodynamic parameters for **14** are reported in Table 4. The values of T_m and $\Delta G°$ are similar to those for the poly(T:A) hairpin **4**, which has two fewer T:A base pairs and no G:G base pair. The more favorable $\Delta H°$ for **14** vs **4** is compensated for by the less favorable $\Delta S°$. Substitution of a G:G base pair for a G:C base pair in RNA duplexes also results in compensating changes in $\Delta H°$ and $\Delta S°$.[25] Smaller decreases in T_m are observed upon introduction of a second or third G:G tandem mismatch in hairpins **15** and **16**. The T_m of **17** which has four tandem mismatches is slightly higher than that of **16** and is similar to that of **13** which also has four G:G base pairs but lacks a poly(T:A) stem region. Thus, the stability of the G:G containing hairpins appears to be determined primarily by the structure of the hairpin loop region.

The CD spectra of **14** and **15** (Figure 5c) are similar to those of the poly(T:A) hairpins and thus are assumed to adopt B-form structures. No negative band for the stilbene diether chromophore is observed around 330 nm. This may indicate that the interaction between the stilbene diether and the adjacent base pair is weaker for G:G than it is for G:C or T:A.

Introduction of a single G:G mismatch in B-DNA is known to result in a significant increase in the helical width.[24] This suggests the possibility that the **Sd2** linker may be too short to optimally span the G:G mismatch in **14**. Conjugate **18** possesses an **Sd4** linker which should be capable of spanning a wider helix (Chart 1). However, the lower T_m value for hairpin **18** vs **14** (Table 2) suggests that the **Sd4** linker may be longer than needed for this purpose. It is interesting to note that the difference in T_m values for **18** vs **14** (50.2 vs 53.4 °C) is smaller than that for **9** vs **5** (56.6 vs 64.2 °C), suggesting that the difference in stability for the shorter vs longer linker is smaller in the case of the wider G:G-containing helix. It would be interesting to determine if more stable hairpins possessing G:G mismatches can be obtained using the **Sd3** linker.

Hairpin Fluorescence and Photoisomerization. Unlike the unmodified stilbene diether linkers which are strongly fluores-

(21) (a) Varani, G. *Annu. Rev. Biophys. Biomol. Struct.* **1995**, *24*, 379−404. (b) Yoshizawa, S.; Kawai, G.; Watanabe, K.; Miura, K.; Hirao, I. *Biochemistry* **1997**, *36*, 4761−4767.
(22) Basham, B.; Eichman, B. F.; Ho, P. S. In *Oxford Handbook of Nucleic Acid Structure*; Neidle, S., Ed.; Oxford: Oxford, UK, 1999.
(23) Chattophdhyaya, R.; Grzeskowiak, K.; Dickerson, R. E. *J. Mol. Biol.* **1990**, *211*, 189−197.
(24) Skelly, J. V.; Edwards, K. J.; Jenkins, T. C.; Neidle, S. *Proc. Natl. Acad. Sci. U.S.A.* **1993**, *90*, 804−808.
(25) Burkard, M. E.; Turner, D. H. *Biochemistry* **2000**, *39*, 11748−11762.
(26) Huertas, D.; Azorín, F. *Biochemistry* **1996**, *35*, 13125−13135.
(27) Lewis, F. D.; Wu, Y.; Liu, X.; Zhang, L. Unpublished results.

cent (Table 1), hairpins **1**−**12** are very weakly fluorescent ($\Phi_{fl} < 10^{-2}$). For example, the fluorescence quantum yields for hairpins **5** and **12** are 7×10^{-3} and 5×10^{-3}, respectively. Their fluorescence excitation and emission spectra are similar to those for hairpin **13** (Figure 6). The weak fluorescence of hairpins with adjacent T:A or G:C base pairs has been attributed to electron-transfer quenching in which the stilbene diether serves as an electron donor and either T or C as an electron acceptor.[4] The occurrence of fluorescence quenching via rapid electron transfer is supported by picosecond time-resolved transient absorption spectroscopy, which shows the rapid conversion of the stilbene diether singlet to its cation radical. The free energy of the photochemical electron-transfer process can be estimated using Weller's equation (eq 2), using the **Sd2** singlet excitation energy ($E_s = 3.45$ V) and ground-state oxidation potential ($E_{ox} = 0.92$ eV vs SCE in DMF solution) and the nucleobase oxidation potentials ($E_{rdn} = -2.26$ and -2.36 eV for dT and dC, respectively). In contrast to the exergonic reduction of T or C, reduction of G ($E_{rdn} < -3.0$ eV) is calculated to be endergonic using the single nucleotide reduction potentials in nonaqueous solution. In accord with this calculation, hairpins **13**, **16**, and **17**, which have three or four tandem G:G base pairs, have fluorescence quantum yields similar to those of stilbene diether linkers and somewhat longer singlet decay times (Tables 1 and 3). The lower values of Φ_{fl} and τ_s for hairpins **14** and **15** may reflect quenching by the nearest T:A base pair.

$$\Delta G_{et} = -(E_S + E_{rdn}) + E_{ox} \qquad (2)$$

Hairpin **4** undergoes moderately efficient photoisomerization under denaturing conditions (50% ethanol−water) but not under conditions where it forms a stable hairpin structure. The photostability of **4** and other hairpins in which the **Sd** linker is adjacent to an A:T or G:C base pair may reflect either very rapid electron-transfer quenching or a well-ordered loop geometry (Figure 2b) which inhibits photoisomerization. Irradiation of *c*-**4** under conditions where it forms a stable hairpin structure results in one-way isomerization to yield **4** with a quantum yield of 0.17. Incomplete quenching of the photoisomerization of singlet *c*-**4** might reflect a lower inherent barrier for isomerization of *cis*- versus *trans*-stilbenes or the "looser" geometry of the hairpin loop region of *c*-**4**. A looser loop geometry with poor π-stacking between the cis-linker and adjacent base pair should result both in slower electron-transfer quenching and in a lower barrier to double bond torsion. Photoisomerization of the **Sd2** linker is also observed for hairpins possessing G:G base pairs adjacent to the linker. Both inefficient electron-transfer quenching and a distorted hairpin loop geometry may facilitate the isomerization process.

Concluding Remarks

Bis(oligonucleotide) conjugates possessing a **Sd2** stilbene diether linker are capable of forming remarkably stable hairpins with a variety of base-paired stems. Conjugates possessing only two T:A or G:C base pairs have melting temperatures of 30 and >80 °C, respectively, in 0.1 M NaCl. On the basis of these results, the **Sd2** linker forms more stable hairpins than any synthetic or natural hairpin loop reported to date. The thermal stability of hairpins possessing a **Sd2** linker is attributed to several factors: (a) the rodlike stilbene which reduces the entropy of hairpin formation; (b) the preferred gauche conformation of the flexible 1,2-dioxoethanes which connect the stilbene to the sugar−phosphate backbone; (c) its total length which matches the B-form helix diameter; (d) the π-stacking interaction between the electron-rich stilbene and the electron-poor adjacent base pair. The hairpin *c*-**4**, which possesses a *c*-**Sd2** linker (Figure 2c), is much less stable than hairpin **4**, as a consequence of the nonplanar stilbene which cannot form a π-stacked complex with the adjacent A:T base pair and an end-to-end distance that is shorter than that for the **Sd2** linker. The thermal stability of hairpins with poly(T:A) stems and **Sd3** linkers are similar to those with **Sd2** linkers. Hairpins possessing **Sd4** linkers are less stable, plausibly due to the less favorable entropy for folding the longer polymethylene chains (Figure 2d). All of the conjugates have CD spectra indicative of B-DNA structures, except for **12**, in which the G_3-C_3 stem evidently adopts a left-handed Z-DNA structure.

The stilbene diether linkers also form stable hairpin structures containing noncanonical G:G base pairs. To our knowledge, **13** is the first hairpin-forming conjugate reported to have a poly(G:G) stem. Annealing of **13** results in the formation of more stable quadruplex structures. The formation of stable hairpins is also observed for conjugates **14**−**18**, which contain one or more G:G base pairs between the linker and a poly(T:A) stem. The fluorescence and photoisomerization of the stilbene diether linker is strongly quenched by adjacent T:A or G:C base pairs but not by G:G base pairs. Quenching is proposed to occur via an electron-transfer mechanism in which the singlet stilbene serves as an electron donor and T or C as an electron acceptor. The dynamics of the charge injection process are currently under investigation.

Experimental Section

Bis(2-hydroxyalkyl)stilbene 4,4′-Diethers. The stilbene diether **Sd2** was prepared by the method of Sieber[6] via the reaction of 2-phenoxyethanol with chloroacetaldehyde dimethyl acetal in 1:1 acetic acid−sulfuric acid followed by isolation of the organic product and heating to 200−250 °C on a sand bath. The resulting crystalline solid was recrystallized from pyridine and sublimed prior to use. **Sd3** and **Sd4** were prepared by the analogous reactions of 3-phenoxypropanol and 4-phenoxybutanol, respectively. The former was prepared from the reaction of sodium phenoxide with 3-bromo-1-propanol, and the latter, via the reduction of ethyl 4-phenoxyl-*n*-butyrate with lithium aluminum hydride. Obtained in this fashion were the following:

Bis(2-hydroxyethyl)stilbene 4,4′-Diether (Sd2). Mp: 259 °C (lit.[6] mp 254 °C). ^{1}H NMR (DMSO-d_6): δ 3.55 (m, 4H), 4.04 (t, 4H), 4.56 (t, 2H), 6.91 (d, 4H), 7.02 (s, 2H), 7.48 (d, 4H).

Bis(3-hydroxypropyl)stilbene 4,4′-Diether (Sd3). Mp: 236 °C (lit.[6] mp 221 °C). ^{1}H NMR (DMSO-d_6): δ 1.86 (m, 4H), 3.55 (t, 4H), 4.05 (t, 4H), 4.57 (t, <1H), 6.92 (d, 4H), 7.02 (s, 2H), 7.48 (d, 4H).

Bis(4-hydroxybutyl)stilbene 4,4′-Diether (Sd4). Mp: 203 °C. ^{1}H NMR (DMSO-d_6): δ 1.56 (m, 4H), 1.75 (m, 4H), 3.47 (>4H overlapped with ^{1}H in H_2O), 3.98 (t, 4H), 4.46 (t, ~2H), 6.91 (d, 4H), 7.02 (s, 2H), 7.48 (d, 4H).

Preparation of 4,4′-Dimethoxytrityl Derivatives. The stilbene diethers were converted to their mono(dimethoxytrityl) (DMT) derivatives using the method of Letsinger and Wu.[2] Obtained by this method in 25−40% yield were the following:

Sd2-Mono-DMT. ^{1}H NMR (CD_3Cl): δ 3.43 (t, 2H), 3.8 (s, 6H), 3.95 (t, 2H), 4.15 (m, 4H), 6.82 (d, 4H), 6.92 (m, 6H), 7.2−7.5 (m 13H).

Sd3-Mono-DMT. ^{1}H NMR (CD_3Cl): δ 2.1 (p, 4H), 3.3 (t, 2H), 3.8 (s, 6H), 3.9 (t, 2H), 4.15, 7.45−6.88.

Sd4-Mono-DMT. ^{1}H (CD_3Cl): δ 1.8 (m, 4H), 1.88 (m, 4H), 3.15 (2H), 3.75 + 3.8 (8H), 3.96 (t, 2H), 4.05 (t, 2H), 6.94−6.83 (m, 8H), 7.3−7.5.

Preparation of Phosphoramidite Derivatives. The DMT derivatives were converted to their cyanoethyl-*N*,*N*-diisopropyl phosphoramidite derivatives by the method of Letsinger and Wu.[2] Obtained by this method in 50−70% yield were the following:

Sd2-Mono-DMT-Phosphoramidite. ^{1}H NMR (CD_3Cl): δ 1.2 (d, 12H), 2.6 (t, 2H), 3.45 (t, 2H), 3.65 (m, 2H), 3,80 (s, 6H), 4.18 (m, 4H), 6.9 (m, 10H), 7.2−7.5 (m, 13H). ^{31}P NMR (CD_3Cl, H_3PO_4 as external standard): δ 149.87.

Sd3-Mono-DMT-Phosphoramidite. ^{1}H NMR (CD_3Cl): δ 1.2 (m, 12H), 2.1 (m, 4H), 2.65 (t, 2H), 3.30 (t, 2H), 3.60 (m, 2H), 3,80 (s, 6H), 3.85 (m, 2H), 4.16 (m, 4H), 6.8−6.95 (m, 10H), 7.35 (d, ∼6H), 7.45 (m, 7H). ^{31}P NMR (CD_3Cl, H_3PO_4 as external standard): δ 148.9 (s).

Bis(oligonucleotide) Conjugates. The preparation, purification, and characterization of the bis(oligonucleotide) conjugates **1**−**18** followed the method of Letsinger and Wu[2] as implemented by Lewis et al.[28] Molecular weights of selected conjugates were determined by electrospray ionization mass spectroscopy using a Micromass Quattro II atomospheric pressure ionizaton system. Conjugates were purified using a Nensorb 20 nucleic acid purification cartridge prior to direct loop injection.

Conjugate 1. MS (*m*/*z*): calcd for $C_{135}BrH_{165}N_{44}O_{76}P_{12}$, 4071.65; found, 4071.1 ± 0.15.

Conjugate 5. MS (*m*/*z*): calcd for $C_{138}H_{158}N_{42}O_{76}P_{12}$, 3992.70; found, 3992.61 ± 0.15.

Conjugate 13. MS (*m*/*z*): calcd for $C_{98}H_{108}N_{40}O_{52}P_8$, 2933.68; found, 2933.62 ± 0.12.

Methods. Methods employed for the recording of electronic absorption and fluorescence spectra, determination of fluorescence quantum yields and lifetimes, recording of circular dichroism spectra, and determination of molecular mechanics calculations have been previously described.[28] All spectral data was obtained for solutions of 2×10^{-6} M hairpins in aqueous sodium phosphate buffer (10 mM, pH 7.2) containing 0.1 M NaCl, unless otherwise noted.

Acknowledgment. This research is supported by a grant from the Division of Chemical Sciences, Office of Basic Energy Sciences, U.S. Department of Energy, under Contract DE-FG02-96ER14604. We thank Robert L. Letsinger for stimulating our interest in hairpin-forming DNA conjugates.

JA026941O

(28) Lewis, F. D.; Wu, T.; Liu, X.; Letsinger, R. L.; Greenfield, S. R.; Miller, S. E.; Wasielewski, M. R. *J. Am. Chem. Soc.* **2000**, *122*, 2889−2902.